A BOUNDARY ELEMENT FORMULATION FOR THE SOLUTION OF THE ILL-POSED PROBLEM OF CONTACT STRESS RECONSTRUCTION

Luciano Mendes Bezerra
Comissão Nacional de Energia Nuclear - IPEN/SP
São Paulo - SP - Brasil

ABSTRACT

The state of deformation, strain, and stress within a body may be determined only when a sufficient set of boundary conditions (displacement & traction) is defined. Sometimes, the complete set of boundary tractions may not be available as in the case of contact regions between two bodies. The solution of the Ill-Posed Problem of Contact Stress Reconstruction, despite its numerous physical applications, has received scant attention in the literature so far. Techniques for the solution of such problems, for examples, may be employed in characterizing boundary tractions at inaccessible regions of critical components in sensitive mechanical equipment or to determine tractions in physical truncations needed in partial mesh discretization of a body. The numerical solution of the IPP of CSR simulates the exploitation of a combination of experimental and numerical techniques in a complementary fashion. This paper presents a boundary element formulation with explicit calculation of the sensitivities in an optimization framework for the solution of the IPP of CSR from measurements located at discrete locations of a solid. The magnitude, location,and extent of the contact stresses are defined in terms of load and geometric parameters.

INTRODUCTION

The beginning of the space era has played an important role in the development of numerical solutions for Ill-Posed Problem (IPP) in engineering. It was impossible to place sensors directly on the surface of spacecraft because the aerodynamic heating of reentry vehicles was very severe. It was necessary to embed the sensors beneath the surface of the vehicle. The problem of estimating surface heat flux from interior temperature measurements is known as the Inverse Heat Conduction Problem (IHCP) in the literature [1]. In solid mechanics, the problem of Contact Stress Reconstruction (CSR), based on measurements from sensors located on the boundary or at interior points of the body, constitutes an IPP. This type of problem can be found, for example, in characterizing tractions at inaccessible regions of critical components in sensitive mechanical equipment, or characterizing tractions on a portion of the body embedded in a hazardous environment. Another application is the determination of tractions in a physical truncation such tractions may be needed in a partial mesh discretization of the body. In such cases, the internal data are generally not only more accurate, but easier to assess. Techniques like strain gages, photoelasticity, coating, and speckle interferometry, among others, are reliable experimental methods for the determination of deformation, strain and stress tensors at the boundary of or inside a body [2]. Computational techniques for the solution of the IPP of CSR may provide an evaluation tool for identifying contact regions in neighboring objects, as well as hybrid experimental and numerical methods for the analyses of solids [2,3]. Schnur et al. [4] presented the boundary condition reconstruction for elastostatics application using the FEM in conjunction with spatial regularization.. In this paper, optimization approach was not employed and only magnitudes of simple traction distributions at a fix location on the surface of the body were determined. In the present paper, the IPP of CSR is first explained and expressed in mathematical terms. The problem is then formulated as a constrained nonlinear optimization problem in a BEM framework. Using function specifications for the unknown contact stresses, the solution procedure adopted seeks to minimize the difference between the experimental data and the corresponding computed quantities. Geometric constrains forcing on that CSR lies within a specific portion of the boundary of the body are also imposed. The design sensitivities required in the optimization procedure are obtained by the implicit differentiation [5] of the BEM integral equations. Examples involving the determination of the magnitude, extent, and location of contact stresses are presented in this paper.

DEFINITION OF THE PROBLEM

Consider that in Figure 1 the external boundary Γ of the solid Ω got in touch with another body, and the contact traction Φ has its magnitude, extent, and location unknown. The reconstruction ofΦ, anywhere along the boundary Γ of the solidΩ, based on internal or external experimental data in terms of displacements, stresses, or strains constitutes an IPP. In mathematical notation, this can be expressed as

$$\sigma_{ij,j}(x) = -b_j(x); \quad \forall x \in \Omega \tag{1}$$

$$\sigma_{ij,j}(x) = \lambda \delta_{ij} \varepsilon_{ll}(x) + 2\mu \varepsilon_{ij}(x); \quad \forall x \in \Omega \tag{2}$$

$$\varepsilon_{ij}(x) = \frac{1}{2}\left[u_{i,j}(x) + u_{j,i}(x)\right]; \quad \forall x \in \Omega \tag{3}$$

$$\sigma_{ij}(y) n_i(y) = \bar{t}_i; \quad y \in \Gamma_1 \tag{4}$$

$$u_i(y) = \bar{u}_i; \quad y \in \Gamma_2, \text{ and} \tag{5}$$

$$\hat{\varphi}_{ik} = \varphi_i(x_k); \quad x_k \in \Gamma^*, \text{or } x_k \in \Gamma \tag{6}$$

where x and y are position vectors belonging to the body Ω and to the boundary Γ of the body, respectively. σ_{ij}, ε_{ij} , b_j, u_i, t_i, are; stress, strain, body force, displacement,

and traction, respectively. The overbar quantities $\bar{t}_i$ and $\bar{u}_i$ are prescribed tractions and displacements, respectively. λ and μ are the Lamé's constants, and δ_{ij} is the Kronecker's delta. The quantities $\hat{\varphi}_{ik}$ with $(i = x,y)$ and $(k = 1,2,3...m)$ are simulated experimental quantities along the direction "i" and at location "k." Such experimental quantities $\hat{\varphi}_{ik}$ may be internal or external data in terms of displacements, stresses, or strains. In this paper, $\hat{\varphi}_{ik}$ will be simulated from the solution obtained from a boundary element analysis with the actual contact stress applied. The approach followed in this paper to solve the IPP of CSR is the best-fit method using optimization technique. A residual function that measures the differences between the model prediction and the measured data is minimized. A number of metrics can be employed to express the residual function. In this paper, the residual function $f(z)$ to be minimized is written as the Euclidean norm of the difference between $\hat{\varphi}_{ik}$ and the corresponding computed quantities φ_{ik} multiplyed by a weighting parameter "w" to enhance numerical sensitivity. The vector $\{\hat{\varphi}\}$ refers to the data vector, and the mapping $Az = \{\varphi\}$ corresponds to the computed quantity. $\{\varphi\}$ is obtained in terms of the model vector $z^T = \{z_1, z_2 \cdots z_n\}$, where z_n represents design variables specifying magnitude, extent, and location of the contact stress. The objective function to minimize can be written as

$$f(z) = w \sum_{k=1}^{m} \sum_{i=1}^{2} \left(\varphi_{ik} - \hat{\varphi}_{ik}\right)^2 \qquad (7)$$

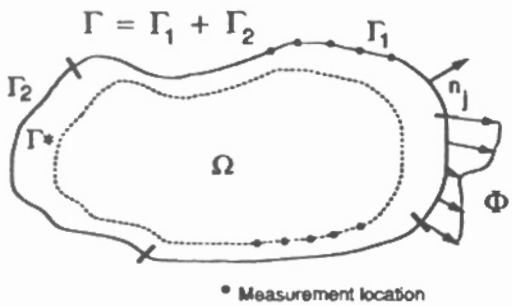

Figure-1: IPP of stress reconstruction

MINIMIZATION OF THE RESIDUAL

The use of numerical methods in conjunction with digital computers has enabled structural engineers in the last decades to solve a wide variety of complex problems. The CSR based on observations around or inside the body involves the determination of the magnitude, extent, and location of the contact stresses acting on Γ and expressed by the model vector $z^T = \{z_1, z_2 \cdots z_n\}$. The numerical procedure adopted in this study for the solution of the IPP of CSR involves the determination of the model vector $z^T = \{z_1, z_2 \cdots z_n\}$ such that the function $f(z)$ in Eq. (7) be a minimum. $f(z)$ is referred to as the residual or objective function to minimize. For the solution of this IPP, suppose that the possible location of the contact stress is limited to a bounded set of locations on the boundary of the body, say on $\overline{\Gamma}_1 \subset \Gamma_1$. Geometric constraints to prevent contact stress from lying out of the feasible region is adopted. The inequalities, denoting the geometric constraints, may be written as $C_j(z_i) \geq 0$. To take $C_j(z_i)$ into account in the minimization process, the internal penalty function method is used since it assures at least a minimum inside the feasible region. Among the internal functions (*infinity*, *log* and *inverse* barrier function), the inverse penalty barrier function has a more desirable behavior because it gradually penalizes the objective function as the search points approach the limits of the feasible region. Making $\Re$ the penalty parameter, the new augmented objective function to be minimized is then given by

$$F(z_i, \Re) = f(z_i) + \Re \sum_{j=1}^{L} \sum_{i=1}^{P} C_j^{-1}(z_i) \qquad (8)$$

A number of methods are available in the literature for the minimization of an objective function $F(z_i) = F(z_i, \Re)$. Of broad use are the methods of *first-order*, such as the variable metric method which is a quasi-Newton method, and is considered to be a powerful optimization method [7]. In the variable method, for a fix $\Re$, it is postulated that $F(z_i)$ may be locally approximated, at any point $\tilde{z}$, by a Taylor's expansion

$$F(z) = F(\tilde{z}) + \sum_{i} \frac{\partial F(\tilde{z})}{\partial z_i}(z - \tilde{z}) + \sum_{i,j} \frac{\partial^2 F(\tilde{z})}{\partial z_i z_j}(z - \tilde{z})^2 + \cdots \qquad (9)$$

In matrix notation and including terms up to the quadratic order, Eq. (9) can be rewritten as

$$F(z) \approx A + Bz^T + \frac{1}{2} z H z^T \qquad (10)$$

where the matrix A is a constant, B is the gradient vector, and the matrix of the second order derivatives, H, is called the *Hessian* of the function $F(z_i)$. Taking the derivatives of Eq. (10), the gradient of the function $F(z)$ is $\nabla F(z) = Hz - B$. The variable metric methods attempt to iteratively build up a good approximation to the inverse of the *Hessian* matrix H^{-1}. That is, it constructs, during an infinity number of iterations $(k \to \infty)$, a sequence of matrices $\aleph^{(k)}$ that will converge to the inverse of H^{-1}. If the minimum of $F(z_i)$ is achieved in N finite number of iterations, then $\aleph^{(k)}$ can be used to update the vector z. Suppose that z^* gives the minimum of $F(z_i)$, then $\nabla F(z^*) = Hz^* - B = 0$. At any iteration $z^{(k)}$, we can write $Hz^{(k)} = \nabla F(z^{(k)}) - B$. Subtracting this equation from the firts one, and multiplying the resultant expression by the inverse of the *Hessian* matrix H^{-1}, *it yields*

$$z^* - z^{(k)} = -H^{-1}\left[\nabla F(z^{(k)})\right] \qquad (11)$$

The left-hand side of Eq. (11) represents a finite step needed to take the vector $z^{(k)}$ towards the exact minimum z^*. Subtracting Eq. (11) at $z^{(k+1)}$ from the same equation at $z^{(k)}$ gives

$$z^{(k+1)} - z^{(k)} = -H^{-1}\left[\nabla F(z^{(k+1)}) - \nabla F(z^{(k)})\right] \qquad (12)$$

In the variable metric method, the sequence $\aleph^{(0)}, \aleph^{(1)}, \aleph^{(2)}, \ldots, \aleph^{(k+1)}$ approaches H^{-1} in a finite number of

iterations. In this paper, the recursive formulae from the BFGS algorithm (due to Broyden, Flecher, Goldfarb, and Shanno) are applied to update $\aleph^{(k+1)}$[6]. Substituting in Eq. (12) H^{-1} for $\aleph^{(k+1)}$, and adopting the abbreviation $S(z^{(k)}) = S^{(k)} = \aleph^{(k+1)}\left[\nabla F(z^{(k+1)}) - \nabla F(z^{(k)})\right]$ then, if we start from an initial guess defined by the vector $z^{(0)}$, the update of the vector $z^{(k)}$ in search of the minimum in the direction $S^{(k)}$ can be written as

$$z^{(k+1)} = z^{(k)} + \alpha^{(k)} S^{(k)} \qquad (13)$$

where $\alpha^{(k)}$ is the step-length along a line search direction. In the sub-minimization process of finding the appropriated $\alpha^{(k)}$ to minimize $F(z) = F(z, \Re)$, given the initial guess $z^{(0)}$, the derivatives of $F(z^{(0)})$ and the search direction $S^{(0)}$ are calculated. Three values $\alpha^{(a)} < \alpha^{(b)} < \alpha^{(c)}$ corresponding to three points $z^{(a)} < z^{(b)} < z^{(c)}$ in Eq. (15), along the path $S^{(0)}$, are found. These points are such that $F(z^{(a)}) > F(z^{(b)}) < F(z^{(c)})$. To ensure that the location of the vector $z^{(k)}$ lies inside the feasible domain $\overline{\Gamma}_1 \subset \Gamma_1$, the step-length $\alpha^{(k)}$ is successively contracted by 10%, when necessary, until $z^{(k)}$ lies inside the feasible domain. With the three initial points $\alpha^{(a)} < \alpha^{(b)} < \alpha^{(c)}$, Brent's method [7] is applied to find the minimum of $F(z)$ along $S^{(0)}$ by approximating the function $F(z)$ by a parabola fitted through $\left\{\alpha^{(a)}, \alpha^{(b)}, \alpha^{(c)}\right\}$. With $F^{(a)} = F(z^{(a)})$, $F^{(b)} = F(z^{(b)})$, and $F^{(c)} = F(z^{(c)})$, solving the inverse interpolation problem, the variable $\alpha^{(m)}$ denoting the minimum of the interpolating parabola, is found as

$$\alpha^{(m)} = \alpha^{(b)} + \frac{\left(\alpha^{(b)} - \alpha^{(a)}\right)^2\left[F^{(b)} - F^{(c)}\right] - \left(\alpha^{(b)} - \alpha^{(c)}\right)^2\left[F^{(b)} - F^{(a)}\right]}{\left(\alpha^{(b)} - \alpha^{(a)}\right)\left[F^{(b)} - F^{(c)}\right] - \left(\alpha^{(b)} - \alpha^{(c)}\right)\left[F^{(b)} - F^{(a)}\right]} \qquad (14)$$

The above relation fails only if the three points are collinear. Brent's method takes care of this situation by shifting the search for the minimum to the Golden Section method [7] whenever necessary. At the minimum $\alpha^{(m)}$, $F(z^{(m)})$ is evaluated. $F(z^{(a)})$, $F(z^{(b)})$, and $F(z^{(c)})$ are compared with $F(z^{(m)})$ and the one with the most difference is replaced by $F(z^{(m)})$. Thus, a new triple set of points is obtained. A parabola is fitted through this new set of points, and the process is iteratively applied until the minimum of the function $F(z)$ in the search direction being pursued is found. Upon determining the appropriate $\alpha^{(k)}$ that minimizes $F(z)$ in the search direction corresponding to iteration "k," the BFGS algorithm is applied to update $\aleph^{(k+1)}$, $S^{(k+1)}$, and $z^{(k+1)}$. A check for convergence is performed, if convergence has been achieved the program stops. If convergence has not been achieved, the next iteration begins with the updated values of $\aleph^{(k+1)}$, $S^{(k+1)}$, and $z^{(k+1)}$.

BEM AND SENSITIVITIES

The most widely used numerical techniques successfully applied to direct problems are the FEM and the BEM[8]. A recent review of the literature indicates that the FEM has been systematically incorporated into numerical schemes for solving IPP [9]. During the last decade, though, the BEM has become an alternative analysis method and has emerged as a powerful tool for solving various complex problems. Despite its shortcomings due to the mathematical complexity underlying the method, there are many advantages that make the BEM an attractive and competitive technique. The BEM has some distictic advantages, especially for certain classes of linear problems over "domain" type techniques such as the FEM. In the BEM the dimensionality of the problem is reduced by one. For example, 2D problems are reduced to line integrals. As a "meshless" method the BEM is well suited for problems involving continuous mesh updates. The contact stress reconstruction is an example of such problem. In the IPP of CSR, the extent and location of the contact stresses acting on Γ have to be found and for that the mesh at the boundary has to be constantly updated. The use of BEM technique makes the mesh update easier. The fundamental equation in the BEM is the Somigliana's identity. Omitting the body force, the Somigliana's identity can be written as

$$u_i = \oint_{\Gamma_1} \overline{u}_{ij}^{*} t_j + \oint_{\Gamma_2} \overline{u}_{ij}^{*} t_j - \oint_{\Gamma_1} \overline{t}_{ij}^{*} t_j - \oint_{\Gamma_2} \overline{t}_{ij}^{*} t_j \qquad (15)$$

$$\text{with} \quad u_i^{*} = c_1\left(c_2 \delta_{ij} \log R - \left(Y_i Y_j\right)/R^2\right) \qquad (16)$$

$$t_{ij}^{*} = \left(c_3/R^2\right)\left[c_4\left(n_k Y_i - n_i Y_k\right) + \left(c_4 \delta_{ik} + \left(2 Y_i Y_k\right)/R^2\right) Y_j n_j\right] \qquad (17)$$

where $u_i^{*} = u_i^{*}(\xi, x)$, $t_{ij}^{*} = t_{ij}^{*}(\xi, x)$, $\mu = E/\left[2(1+\upsilon)\right]$ is the shear modulus, E is the Young's modulus and υ is the Poisson's ratio, $c_1 = -1/\left[8\pi\mu(1-\upsilon)\right]$, $c_2 = 3 - 4\upsilon$, $c_3 = -1/\left[4\pi(1-\upsilon)\right]$, and $c_4 = 1 - 2\upsilon$. The term $Y_i = x_i + \xi_i$ is the distance between the point load x_i on the boundary and the field point ξ_i, $R^2 = Y_i Y_i$; and n_i are the outward normals at boundary Γ. Similar to Eq. (15), the equation to determine the stresses can be written as

$$\sigma_{ij} = \int_{\Gamma}\left[\varepsilon_{ijk}^{*} t_k - \sigma_{ijk}^{*} u_k\right] d\Gamma \qquad (18)$$

$$\text{with} \quad \varepsilon_{ijk}^{*} = \varepsilon_{ijk}^{*}(\xi, x) = (a_3 n_l Y_l / R^4)\left[2 a_2 \delta_{ij} Y_k + 2\nu(\delta_{ij} Y_k + \delta_{ij} Y_k) - 8 Y_i Y_j Y_k / R^2\right] + (a_3/R^2)\left[n_i(2\nu Y_j Y_k / R^2 + a_2 \delta_{jk}) + n_j(2\nu Y_i Y_k / R^2 + a_2 \delta_{ik})\right] + (a_3/R^2)\left[n_k(2 a_2 Y_i Y_j / R^2 - a_4 \delta_{ij})\right] \qquad (19)$$

$$\text{and} \quad \sigma_{ijk}^{*} = \sigma_{ijk}^{*}(\xi, x) = (a_1/R)\left[a_2(\delta_{ik} Y_j + \delta_{jk} Y_i - \delta_{ij} Y_k)/R + 2 Y_i Y_j Y_k / R^3\right] \qquad (20)$$

where $a_1 = -c_1$, $a_2 = c_4$, $a_3 = \mu/[2\pi(1-\nu)]$, $a_4 = 1 - 4\nu$. Knowing the stresses, the strains can be obtained as

$$\varepsilon_{ij}(\xi) = \sigma_{ij}(\xi)/(2\mu) - 2\delta_{ij}\sigma_{II}(\xi)/[2\mu(2\mu + 3\lambda)] \qquad (21)$$

For the discretization of Eq.(15), Γ is approximated by piecewise elements. The geometry, displacements, and tractions

at Γ_i (a piece of the boundary) can be expressed in the discrete coordinates as

$$x_j(\xi) = \sum_{i=1}^{3} h^i(\zeta) x_j^{(i)} \quad (22), \qquad u_j(\xi) = \sum_{i=1}^{3} h^i(\zeta) u_j^{(i)} \quad (23)$$

$$\text{and} \quad t_j(\xi) = \sum_{i=1}^{3} h^i(\zeta) t_j^{(i)} \quad (24)$$

where $x_j^{(i)}$ are the Cartesian coordinates (x, y in 2D Cartesian planes) defining the geometry; $u_j^{(i)}$ is the nodal displacement; $t_j^{(i)}$ is the nodal traction. $x_j^{(i)}$, $u_j^{(i)}$, and $t_j^{(i)}$ are nodal coordinates, displacements and tractions, respectively, at the nodal point "i." $h_j^{(i)}$ are interpolating functions, which are taken as quadratic functions of the natural coordinate ζ. Introducing Eqs. (22), (23), and (24) into Eq. (15) and manipulating the resulting equation as a system of matrix equation with the modal displacements $u_j^{(i)} \in \{U\}$ on one side and the nodal traction $t_j^{(i)} \in \{T\}$ on the other side, we get

$$[F]\{U\} = [G]\{T\} \quad (25),$$

$$\text{with} \quad G_{pq} = \sum_{k=1}^{N_e} \int_{-1}^{+1} [u_{ij}^*][h] J d\zeta \quad (26),$$

$$\text{and} \quad F_{pq} = \sum_{k=1}^{N_e} \int_{-1}^{+1} [t_{ij}^*][h] J d\zeta \quad (27)$$

where G_{pq} and F_{pq} are the terms of the matrices [F] and [G], respectively. The indices "p" and "q" denote node and element, respectively; N_e is the total number of elements in the mesh. G_{pq} and F_{pq} are the interaction coefficients relating node "q" with all the nodes on the surface of the body. The matrix system of Eq. (25) may be rearranged after all the prescribed boundary conditions (tarctions $\bar{t}$ and displacements $\bar{u}$) are imposed. The manipulation of Eq. (25) is done to transfer all the unknowns on the left-hand side and all the known quantities on the right-hand side, resulting in the following equation $[A]\{v\}=\{b\}$, where $\{v\}$ represents the vector of unknowns and $\{b\}$ the vector of known boundary conditions multiplied by some other matrix resulting from the manipulation operations due to the application of the boundary conditions. Upon finding the unknowns in $\{v\}$, the displacements at any location (internal or external points) can be found from Eq. (15). In the same way, applying the boundary values in the discretized form of Eq. (20), the stresses (and by Eq. (23) also the strains) at any point can be calculated. As explained in the section before, the minimization of Eq. (8) by the variable method requires the evaluation of the gradient of $F(z_i) = F(z_i, \Re)$ with respect to $z^T = \{z_1, z_2 \cdots z_n\}$.

$$\frac{\partial F(z)}{\partial z} = \frac{\partial F(z,\Re)}{\partial z} = 2w \sum_{k=1}^{m} \sum_{i=1}^{2} (\varphi_{ik} - \hat{\varphi}_{ik}) \frac{\partial \varphi_{ik}}{\partial z} - \Re \sum_{j=1}^{L} \left[\frac{1}{C_j^2(z)} \frac{\partial C_j(z)}{\partial z} \right] \quad (28)$$

The *Hessian* matrix which is the second derivative of $F(z_i)$ is approximated by the BFGS algorithm. This algorithm, iteratively, builds up a good approximation to the inverse of the *Hessian* and for such it needs only the first-order derivatives of the function $F(z_i)$ in Eq.(28). In that equation, $\partial \varphi_{ik} / \partial z$ are the sensitivities of displacements, strains, and stresses depending on what experimental quantities are used in the data vector $\{\hat{\varphi}\}$. To find $\partial \varphi_{ik} / \partial z$ the first derivatives of the boundary displacements and boundary tractions are needed. To accomplish this, the implicit differentiation of Eq. (25) with respect to the design variable, z, leads to

$$[F]\{U\}_{,z} + [F]_{,z}\{U\} = [G]\{T\}_{,z} + [G]_{,z}\{T\} \quad (29)$$

$$\text{with} \quad G_{pq,z} = \sum_{k=1}^{N_e} \int_{-1}^{+1} \left\{ [u_{ij,z}^*][h] J + [u_{ij}^*][h] J_{,z} \right\} d\zeta \quad (30),$$

$$\text{and} \quad F_{pq,z} = \sum_{k=1}^{N_e} \int_{-1}^{+1} \left\{ [t_{ij,z}^*][h] J + [t_{ij}^*][h] J_{,z} \right\} d\zeta \quad (31)$$

The derivative of the kernels $u_{ij,z}^*$ and $t_{ij,z}^*$ with respect to vector z are, respectively

$$u_{ij,z}^* = u_{ij,z}^*(\xi, x) = c_1 \left[c_2 \delta_{ij} R_{,z} / R - \left(Y_{i,z} Y_j + Y_i Y_{j,z} \right) / R^2 + 2 Y_i Y_j R_{,z} / R^3 \right] \quad (32)$$

$$\text{and} \quad t_{ij,z}^* = t_{ij,z}^*(\xi, x) = \left(c_3 c_4 / R^2 \right) \left(n_j Y_{i,z} + n_{j,z} Y_i - n_i Y_{j,z} - n_{i,z} Y_j \right) + \left(c_3 / R^4 \right) \left[2 Y_i Y_j \left(Y_{k,z} n_k - Y_k n_{k,z} \right) + 2 \left(Y_{i,z} Y_j + Y_i Y_{j,z} \right) Y_k n_k - 8 Y_i Y_j Y_k n_k R_{,z} / R \right] - \left(2 c_3 / R^3 \right) \left[c_4 \left(n_j Y_i - n_i Y_j \right) - \left(c_4 \delta_{ik} + \left(2 Y_i Y_j \right) / R^2 \right) \right] R_{,z} \quad (33)$$

where $R_{,z} = R^{-1} Y_k Y_{k,z}$, $n_{2,z} = J^{-2} J_{,z} x_{1,z} + J^{-1} x_{1,z}$, and $n_{1,z} = -J^{-2} J_{,z} x_{2,z} + J^{-1} x_{2,z}$. The singularities in the evaluation of the sensitivities $G_{pq,z}$ and $F_{pq,z}$ have been studied by [5]. Knowing the matrices $[G]_{,z}$ and $[F]_{,z}$ and manipulating Eq. (29) we can write that $[F]\{U\}_{,z} = [G]\{T\}_{,z} + \{r\}$ with $\{r\} = [G]_{,z}\{T\} - [F]_{,z}\{U\}$. After applying the sensitivity (derivative) boundary conditions in that equation one arrives to $[A]\{v\}_{,z} = \{d\} + \{r\}$, where $\{v\}_{,z}$ contains both the boundary displacement and boundary traction derivatives. With the derivatives at the boundaries, the displacement, stress, and strain sensitivities at any field point, can be found through the derivatives of Eqs. (15), (18), and (21), respectively. The derivative of Eq. (15) needs the kernels' sensitivities as expressed in Eqs. (32) and (33). The stress sensitivity (derivative of Eq. (18)) needs the strain and stress kernel derivatives as follows

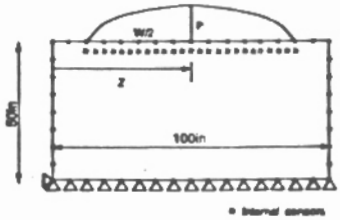

Figure-2: Panel with contact stress to be reconstructed

$$\sigma^{*}_{ijk,x} = \sigma^{*}_{ijk,x}(\xi,x) = -(a_1 R_{,x}/R^3)\left[a_2(\delta_{ik}Y_j + \delta_{jk}Y_i - \delta_{ij}Y_k) + 2Y_iY_jY_k/R^2\right] + (a_1/R^2)\left[a_2 R_{,x}(\delta_{ik}Y_j + \delta_{jk}Y_i - \delta_{ij}Y_k)/R + a_2(\delta_{ik}Y_{j,x} + \delta_{jk}Y_{i,x} - \delta_{ij}Y_{k,x})/R + 2Y_{i,x}Y_jY_k/R^3 + 2Y_iY_{j,x}Y_k/R^3 + 2Y_iY_jY_{k,x}/R^3 + 6R_{,x}Y_iY_jY_k/R^3\right] \quad (34)$$

$$\varepsilon^{*}_{ijk,x} = \varepsilon^{*}_{ijk,x}(\xi,x) = -4(a_3 n_{l,x}Y_l/R^4) (a_3 n_l Y_{l,x}/R^4)(a_3 n_l Y_l R_{,x}/R^5)\left[2a_2\delta_{ij}Y_k + 2\nu(\delta_{ik}Y_j + \delta_{ik}Y_i) - 8Y_iY_jY_k/R^2\right] + (a_3 n_l Y_l/R^4) \left[2a_2\delta_{ij}Y_{k,x} + 2\nu(\delta_{ij}Y_{j,x} + \delta_{ij}Y_{k,x}) - (8/R^2)(Y_{i,x}Y_jY_k + Y_iY_{j,x}Y_k + Y_iY_jY_{k,x} + R_{,x}Y_iY_jY_k/R\right] - (2R_{,x}a_3/R^3) \left[n_i(2\nu Y_jY_k/R^2 + a_2\delta_{jk}) + n_j(2\nu Y_iY_k/R^2 + a_2\delta_{ik})\right] + (a_3/R^2) \left[n_{i,x}(2\nu Y_jY_k/R^2 + a_2\delta_{jk}) + (2\nu n_i/R^2)(Y_{j,x}Y_k + Y_jY_{k,x} - 2R_{,x}Y_iY_k/R) + n_{i,x}(2\nu Y_jY_k/R^2 + a_2\delta_{jk}) + (2\nu n_i/R^2)(Y_{j,x}Y_k + Y_jY_{k,x} - 2R_{,x}Y_iY_k/R)\right] - (2a_3R_{,x}/R^3) \left[n_k(2a_2Y_iY_j/R^2 - a_4\delta_{ij})\right] + (a_3/R^2)\left[n_{k,x}(2a_2Y_iY_j/R^2 - a_4\delta_{ij}) + (2a_2n_k/R^2)(Y_{i,x}Y_j + Y_iY_{j,x} - 2R_{,x}Y_iY_j/R)\right] \quad (35)$$

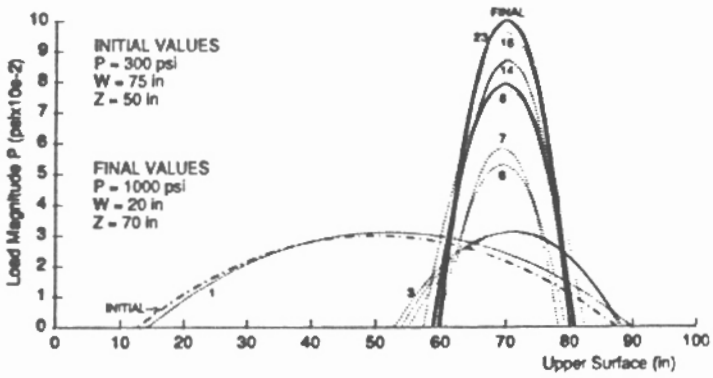

Figure-3: Parabolic contact stress reconstruction

When strains are the measured quantities in the data vector, the strains sensitivities are needed in the minimization process. Knowing the stress sensitivities, the strain sensitivities can be obtained by deriving Eq.(21) w.r.t. vector $\mathbf{z}$.

NUMERICAL EXAMPLES

Two simple example problems are considered to evaluate the formulation presented for IPP of CSR in this paper. In the following examples, the experimental data vector $\hat{\varphi}_{ik}$ will be stresses and strains, respectively, for the first and second example. The data vector were obtained from a priori direct BEM analysis with the actual boundary tractions imposed on the structures. These boundary tractions also served as the "exact" solution for the purposes of comparison of the accuracy of the present procedures.

A panel under parabolic tractions: A simply supported panel, shown in Fig. 2 is considered to get in touch with another structure. The panel has modulus of elasticity, $E = 18.6 \times 10^6 \text{psi}$, and Poisson's ratio, $\nu = 0.3$. At 39 internal sensors (solid crosses at Fig. 2) the state of stress along "x-y" direction is observed while the panel is subjected to an "unknown" normal contact stress with a parabolic distribution at its top edge. The location, Z, the span, W, and the peak magnitude, P, of the parabololic contact stress distribution are unknown and are desired to be reconstructed. Therefore, the model vector $\mathbf{z}^T = \{Z, W, P\}$. The normal distribution of the parabolic contact stress may be expressed as $\sigma(s) = (-4P_s^2 + 8PZs + PW^2 - 4PZ^2)/W^2$, where "s" is the distance along the span of the parabola and $(Z-0.5W) \le s \le (Z+0.5W)$. The initial guess for $\mathbf{z}^T$ was selected to be $\mathbf{z}^T = \{50\text{in}, 75\text{in}, 300\text{psi}\}$. The evolution of the missing traction distribution starting from the initial guess, as the iteractions in the present analysis proceed, is shown in Fig. 3 and 4. The exact traction distribution for this case is also shown in bold line in that figure. As the missing contact stress varied in position and span length after each iteration, the BEM mesh for the upper boundary edge was modified to acommodate such evolutions. The penalty parameter $\Re$ in Eq.(8) was varied during the analysis changing from a value of 10^5 at the beginning to zero at the end. The final solution was obtained in 26 iterations. Table 1 shows the final results obtained with no error in the data vector and also with 5% and 10% random error contaminating the data vector.

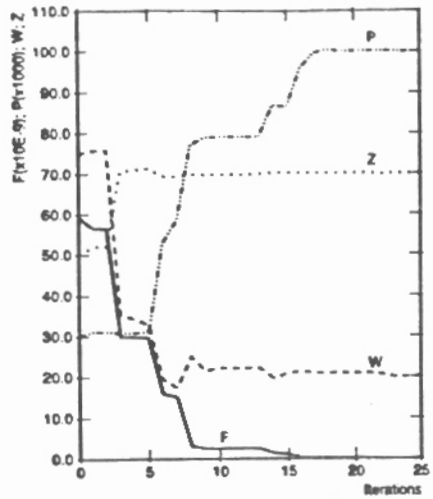

Figure-4: Convergence history of P, W, and Z

A roller under normal and tangential stresses: The contact stresses acting on a roller at its interface with the workpiece are analyzed. The geometry of the roller is represented in Fig. 5. The roller material has $E = 1217 N/mm^2$ and Poisson's ratio $\nu = 0.3$. The boundary region coming in contact with the workpiece was discretized with a finer mesh. The measurements were obtained at 25 internal locations identified by solid crosses at Fig. 4. The data vector in this case consists of strains read at the 25 intrenal locations. The contact region is characterized by the angle "γ". The normal traction distribution is assumed to be symmetric and the tangential traction assumed antisymmetric. They are assumed to be $N(\kappa) = A\sin[\kappa\gamma]$ and $T(\kappa) = B\sin[(\kappa - 0.5)\gamma]$, respectively. A and B are amplitudes of the corresponding traction distribution assumed. In Fig. 6, the residual function to minimize is shown and the region of the minimum can be easily identified. The parameters A, B, and γ define the missing traction distributions and constitute the model vector $\mathbf{z}^T$ for this case. Starting with $A = 55N/mm^2$, $B = 5N/mm^2$, and $\gamma = 10°$, the normal and tangential contact stress converges to the final solution after 18 iterations and are shown in Fig. 7 and 8, respectively.

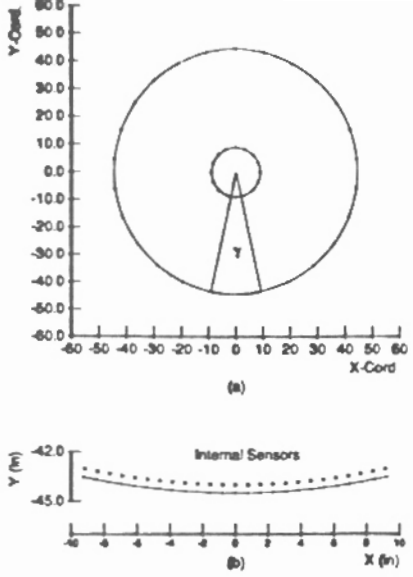

Figure-5: (a)Roller geometry, (b) sensors locations

Tabela 1: Panel with Parabolic Contact Stress

Data Error Parameter	Standard Deviation	Traction N(psi)	Span W(in)	Position Z(in)
$\bar{\eta}$=0%	$\bar{\sigma}$=0.00	1000.1	19.99	70.00
$\bar{\eta}$=5%	$\bar{\sigma}_1$ = 1.38 $\bar{\sigma}_2$ = 3.15	1001.1	19.97	71.11
$\bar{\eta}$=10%	$\bar{\sigma}_1$ = 2.76 $\bar{\sigma}_2$ = 6.31	1001.8	19.94	71.11

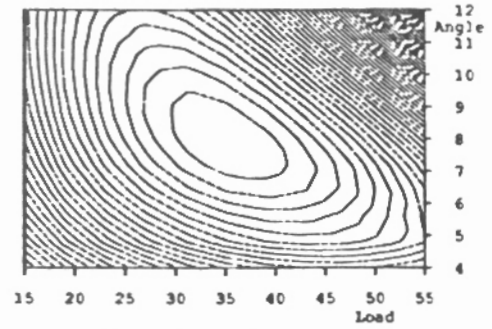

Figure-6: Function contour

CONCLUSIONS

An optimization-based boundary integral formulation for the solution of the ill-posed problem of contact stress reconstruction has been presented. The approach to reconstruct contact stress is based on the minimization of the residual between "experimental" data at discrete points and the corresponding computed quantities. To keep the solution in feasible domains, constraint equations are imposed. The inverse penalty function was augmented to the objective function so that the constrained problem was transformed into an unconstrained one. The minimization is performed using a quasi-Newton method with implicit differentiation of the kernels of the boundary element integral equations. Parabolic and sinusoidal stress distributions were assumed for the unknown contact stress. In this paper, the magnitude, extent, and location of the unknown contact stresses were closely predicted demostrating the validity of the present approach to reconstruct contact stress from "experimental" data. A prime limitation of the present approach arises from the fact that the optimization procedure may converge to a local minimum.

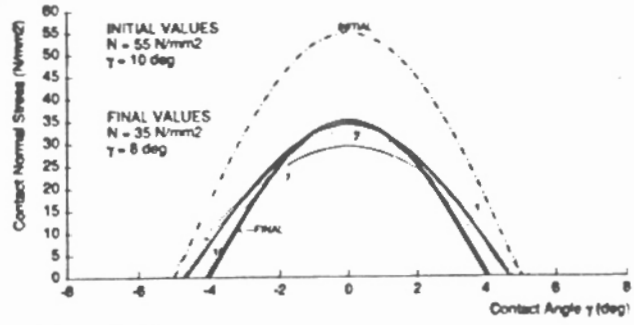

Figure-7: Evolution of normal contact stress-3variables

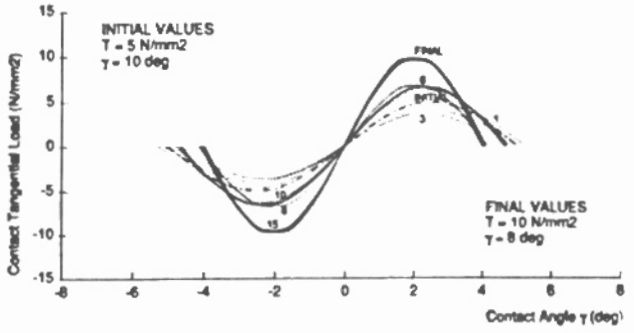

Figure-8: Evolution of tangential contact stress-3variables

REFERENCES

[1] Beck J. V., B. Blackwell, and C. R. StClair Jr. 1985. Inverse Heat Conduction - Ill-posed Problems. New York: Wiley-Interscience Publication.

[2] Weathers J. M., W. A. Foster, W. F. Swinson, and J. L. Turner. 1985. Integration of laser-speckle and finite element techniques of stress analysis. Experimental Mechanics. 25: 60-65.

[3] Balas, J., J. Sladek, and M. Drzik. 1983. Stress analysis by combination of holographic interferometry and boundary integral methods. Experimental Mechanics, 23: 196-202.

[4] Schnur D. S., and N. Zabaras. 1990. Finite element solution of two-dimensional inverse elastic problem using spatial smoothing. Int. J. for Num. Methods in Eng., 30: 57-75.

[5] Saigal S., R. Aithal, and J. H. Kane. 1989. Conforming boundary elements in plane elasticity for shape design sensitivity. Int. J. for Num. Methods in Eng., 28: 2795-2911.

[6] Reklaits G. V., A. Ravindran, and K. M. Ragsdell. 1983. Engineering Optimization - Methods and Applications. New York: John Wiley.

[7] Press W. H., B. P. Flannery, S. A. Teukolsky, and W. T.Vetterling. 1986. Numerical Recipes. New York: Cambridge University Press.

[8] Brebbia C. A., J. C. Telles and L. C. Wrobel. 1984. Boundary Elements Techniques - Theory and Applications in Engineering. Berlin: Spring-Verlag.

[9] Bezerra L. M. 1993. Inverse Elastostatics Solutions With Boundary Elements. PhD Thesis. Carnegie Mellon University. Pittsburgh, PA.